

1 **Title**

2 Stimulus-dependent delay of perceptual filling-in by microsaccades

3 Short title: Stimulus-dependent delay of filling-in.

4  
5 **Authors**

6 Max Levinson<sup>1\*</sup>, Christopher C. Pack<sup>1</sup>, Sylvain Baillet<sup>1\*</sup>

7  
8 **Affiliations**

9 <sup>1</sup> Montreal Neurological Institute, McGill University,  
10 Montreal, Quebec, Canada, H3A 2B4.

11 \* Corresponding authors: max.levinson@mail.mcgill.ca, sylvain.baillet@mcgill.ca

12  
13 **Manuscript Attributes**

14 Number of Pages: 27

15 Number of Figures: 3

16 Number of Tables: 4

17 Number of Words, Abstract: 193

18 Number of Words, Introduction: 561

19 Number of Words, Discussion: 1239

20  
21 **Acknowledgments**

22 This research was supported by the following sources of funding:

23 Quebec Bio-imaging Network project 12.49 (ML)

24 National Sciences and Engineering Research Council of Canada discovery grant RGPIN-2020-  
25 06889 (SB)

26 Canadian Institutes of Health Research Canada Research Chair Tier 1; CRC-2017-00311 (SB)

27 National Institutes of Health grant R01-EB026299 (SB)

28  
29 **Conflict of Interest:** The authors declare no competing financial interests.

30  
31  
32  
33  
34

35 **Abstract**

36 Perception is a function of both stimulus features and active sensory sampling. The illusion of  
37 *perceptual filling-in* occurs when eye gaze is kept still: visual boundary perception may fail,  
38 causing adjacent visual features to remarkably merge into one uniform visual surface.  
39 Microsaccades—small, involuntary eye movements during gaze fixation—counteract perceptual  
40 filling-in, but the mechanisms underlying this process are not well understood. We investigated  
41 whether microsaccade efficacy for preventing filling-in depends on two boundary properties,  
42 color contrast and retinal eccentricity (distance from gaze center). Twenty-one human participants  
43 (male and female) fixated on a point until they experienced filling-in between two isoluminant  
44 colored surfaces. We found that increased color contrast independently extends the duration  
45 before filling-in but does not alter the impact of individual microsaccades. Conversely, lower  
46 eccentricity delayed filling-in only by increasing microsaccade efficacy. We propose that  
47 microsaccades facilitate stable boundary perception via a transient retinal motion signal that  
48 scales with eccentricity but is invariant to boundary contrast. These results shed light on how  
49 incessant eye movements integrate with ongoing stimulus processing to stabilize perceptual  
50 detail, with implications for visual rehabilitation and the optimization of visual presentations in  
51 virtual and augmented reality environments.

52  
53 **Significance Statement**

54 To perceive, sense organs actively sample the environment—for example, by touching, sniffing,  
55 or moving the eyes. Visual sampling persists even when gaze is fixed on a single point:  
56 involuntary microsaccades continuously move the eye in small jumps. We investigated a  
57 previously documented observation that microsaccades prevent illusory fading of perceived visual  
58 boundaries during fixation. We discovered that despite being connected, microsaccades and  
59 fading are sensitive to different stimulus features. Boundaries separating surfaces with more  
60 distinct colors inherently took longer to fade. Boundaries closer to the center of vision also took  
61 longer to fade, but only because microsaccades were more effective. These findings reveal new  
62 insight into how pervasive sensory sampling delivers a stable and detailed perceptual experience.

63  
64  
65 **Keywords**

66 Visual perception, Microsaccades, Fixational eye movements, Visual fading, Perceptual filling-in,  
67 Active vision, Cortical adaptation.

## 70 MAIN TEXT

71

### 72 Introduction

73 When the eyes remain still for an extended period of time, visual boundaries seemingly fade from  
74 view. Boundary fading due to neuronal adaptation (Clarke & Belcher, 1962; Martinez-Conde &  
75 Macknik, 2017; Kohn, 2007) is the first stage of the illusory phenomenon of *perceptual filling-in*,  
76 whereby distinct visual regions appear to merge into a singular, uniform field (De Weerd et al.,  
77 1998; Weil & Rees, 2011). Despite persistent scientific interest in visual fading and filling-in as  
78 consequences of failed perceptual stability, a comprehensive understanding of their underlying  
79 mechanisms remains elusive.

80

81 An important clue comes from observations that microsaccades—small, rapid, and mostly  
82 involuntary eye movements that occur during periods of gaze fixation—inhibit filling-in (Clarke &  
83 Belcher, 1962; Martinez-Conde et al., 2006; Troncoso et al., 2008; McCamy et al., 2012; Costela  
84 et al., 2017). The role of microsaccades in everyday vision is a matter of ongoing debate (Kowler  
85 & Steinman, 1980; Martinez-Conde & Macknik, 2017; Poletti & Rucci, 2010), and it has been  
86 argued that this intriguing laboratory finding is an evolutionary artifact (Collewijn & Kowler, 2008;  
87 Rucci & Poletti, 2015). However, such controlled conditions can offer valuable insights into  
88 microsaccadic impacts on perception, especially related to the neural processes supporting  
89 perceptual stability. Understanding how microsaccades contribute to visual stability could inform  
90 the development of interventions for individuals with impaired visual function, such as those with  
91 age-related macular degeneration or other central vision loss conditions. Additionally, the insights  
92 gained from this study could help optimize visual displays in augmented and virtual reality  
93 environments in the context of naturalistic eye movement patterns.

94

95 The precise mechanism through which microsaccades counteract filling-in is not well understood.  
96 Crucially missing is an account of how stimulus characteristics—such as boundary eccentricity and  
97 contrast—interact with microsaccade efficacy for delaying filling-in, given that, for unclear  
98 reasons, stronger boundaries take longer to fade (Levinson & Baillet, 2022; Weil & Rees, 2011). It  
99 is often proposed that microsaccades serve to "refresh" visual stimuli (Engbert, 2006; Martinez-  
100 Conde et al., 2006), suggesting they generate cortical signals akin to visual stimulation but of  
101 reduced intensity. If so, microsaccades should be more effective over a more pronounced boundary.  
102 Alternatively, microsaccades might influence adapting neurons in unique ways, as they introduce  
103 minor retinal motion and alter the spatiotemporal configuration of the retinal image (Rucci &

Victor, 2015). To examine the interplay between stimulus properties and microsaccade efficacy we developed a perceptual filling-in task based on the Uniformity Illusion (Otten et al., 2016) and analyzed microsaccade dynamics. Participants fixated their gaze until they perceived the merging of a central disk and the surrounding periphery. The circular boundary differed across trials along two axes of boundary strength: isoluminant color contrast and retinal eccentricity.

Using linear mixed modeling, we quantified how stimulus properties and microsaccades interact to influence perceptual stability. Our results demonstrate that microsaccade efficacy in delaying perceptual filling-in is influenced by boundary eccentricity but not by color contrast. Specifically, microsaccades were more effective at lower eccentricities, while color contrast independently extended the time required for perceptual filling-in. The findings suggest that microsaccades do not merely recreate initial stimulus features, but instead prevent perceptual filling-in by transiently refreshing visual signals in a manner dependent on cortical magnification. This study provides new insights into the mechanisms underlying perceptual stability and the role of incessant eye movements in visual processing, with implications for both basic neuroscience and clinical applications.

## Methods

### Participants

Twenty-four participants (14 females, age range: 19-45 years, all right-handed, including one author [ML]) took part in the study. All participants provided written informed consent before participation and were compensated \$30 CAD per hour for their time. The study was conducted under the approval of the McGill University Health Centre Research Ethics Board (protocol 2021-7130). All participants were neurologically healthy and had normal or corrected-to-normal vision. Three participants were excluded before completing their first experimental session: two due to technical issues with the eye-tracking equipment and one due to difficulty maintaining fixation. Consequently, data from 21 participants were analyzed. One participant (subject 203) completed only 8 of the 9 task blocks.

The target sample size was determined by tripling the number of participants—8—included in the seminal study showing that microsaccades counteract visual fading (Martinez-Conde et al., 2006). Our final sample is larger than those in subsequent studies replicating this effect (Costela et al., 2017; McCamy et al., 2012; Troncoso et al., 2008).

138

## 139 **Stimuli and Task**

140 The visual stimulus consisted of a central purple disk (the "center") surrounded by a greyer  
141 rectangular background (the "periphery"). The entire display was contained within a 40.3 x 22.7-  
142 degree rectangular frame centered on the screen. The center and periphery were separated by a  
143 circular boundary, with a width equal to 12% of the center's radius, allowing for a seamless  
144 transition between the two colors.

145

146 Participants completed 450 trials, divided into nine blocks of 50 trials each. At the start of each  
147 trial, participants pressed the spacebar to begin. A fixation target, designed to minimize fixational  
148 eye movements (Thaler et al., 2013), appeared for one second before the onset of the stimulus.

149

150 Participants were instructed to fixate on the fixation cross, minimize blinking, and press the  
151 spacebar once they perceived the center boundary fade and the two colored regions merge into one  
152 uniform color. Participants were informed that this was an illusion and that no physical changes  
153 would occur on the screen. The stimulus disappeared either 1 second after the spacebar press or  
154 automatically after 20 seconds from stimulus onset if no response was given. After each trial,  
155 dynamic colored noise was displayed for a duration equivalent to half of the stimulus presentation  
156 time to alleviate retinal fatigue and after-images.

157

158 Each trial block was defined by a specific combination of color contrast and boundary eccentricity,  
159 with block order randomized for each participant. This ensured that all trials within a block were  
160 identical, preventing interference from after-images of previous trials. Boundary eccentricity was  
161 determined by the radius of the center disk, measured in visual angle, with three sizes: 2 degrees  
162 (small), 4 degrees (medium), and 6 degrees (large). The stimulus color scheme was defined using  
163 an estimation of DKL color space (Derrington et al., 1984), enabling chromatic modulation  
164 measured in degrees around an isoluminant plane. In this DKL plane, all color values maintained a  
165 consistent radius of 0.07 and an elevation of 0 relative to a neutral grey baseline (RGB 77,77,77).  
166 Color contrast was quantified as the difference between the central and peripheral hues, specifically  
167 their DKL azimuth values. The center color was fixed at an azimuth of 270 degrees (RGB 77,75,83),  
168 while the peripheral hue varied across three azimuth values: 280 degrees (low contrast; RGB  
169 83,73,82), 290 degrees (medium contrast; RGB 88,71,82), and 300 degrees (high contrast; RGB  
170 92,69,82). RGB values were converted from DKL using the Computational Colour Science  
171 Toolbox 2e (Westland, 2021) and custom MATLAB code.

172

173 Each block included 50 trials: 40 “main” trials and 10 randomly distributed catch trials. Five of  
174 these catch trials were “replay” trials, which simulated the perceptual filling-in experience to  
175 validate participants’ accuracy in reporting filling-in events. During replay trials, the hues of the  
176 central and peripheral regions gradually merged into a uniform color over 2 seconds, with the onset  
177 of this effect occurring randomly between 4 and 6 seconds after stimulus presentation, following a  
178 uniform distribution.

179

180 The remaining five catch trials were “sharp” control trials, in which the boundary between the  
181 center and periphery was distinct, reduced to a single pixel's width to create a sharp, well-defined  
182 edge. These trials aimed to confirm that a very pronounced boundary would be more resistant to  
183 fading, potentially leading to longer fixation times before participants perceived the merging of the  
184 two regions.

185

### 186 **Isoluminance Calibration**

187 As a preliminary step, we ensured that the different stimulus colors were perceived as isoluminant  
188 by each participant. Isoluminance calibration was conducted using heterochromatic flicker  
189 photometry. During this procedure, a flickering circle with a radius of 200 pixels (approximately  
190 4.2 degrees of visual angle) was displayed at the center of the screen. This circle alternated between  
191 the central hue (purple) and one of the peripheral hues at a frequency of 15 Hz, set against a grey  
192 background of fixed luminance (RGB 77,77,77). Participants adjusted the RGB values of the  
193 peripheral hue using the arrow keys on their keyboard, with goal of minimizing the flicker until it  
194 was either invisible or least noticeable.

195

196 This calibration was repeated for each of the three peripheral hues corresponding to the study’s  
197 three levels of color contrast. A majority of the 21 analyzed participants found the default peripheral  
198 colors to be isoluminant: 81% for low contrast, 76% for medium contrast, and 67% for high  
199 contrast. For participants who required adjustments, the changes were minimal, with average  
200 deviations from the default RGB values being low across all contrast levels:  $1 \pm 0$  (low contrast),  
201  $1.4 \pm 0.89$  (medium contrast), and  $1.43 \pm 0.79$  (high contrast).

202

203 This careful calibration ensured that any observed differences in filling-in time during the main task  
204 were due to the intended properties of the visual boundary and microsaccade dynamics, rather than  
205 variations in stimulus luminance.

206

## 207 **Experimental Procedure**

208 The experiment consisted of three sessions, each scheduled on separate days within a two-week  
209 period. During the first session, participants received both written and oral instructions, followed  
210 by a practice session of 10 trials at medium contrast and eccentricity to familiarize them with the  
211 task.

212

213 Participants completed three task blocks per session. They sat in a dimly lit room with their head  
214 stabilized in a chinrest, positioned 60 cm away from a 27-inch monitor (resolution: 2560 x 1440  
215 pixels; refresh rate: 60 Hz). Visual stimuli were generated using *Psychtoolbox3* (Brainard, 1997) in  
216 MATLAB R2020b (The MathWorks Inc., 2020). Eye movements were recorded at a 1000-Hz  
217 sampling rate with an EyeLink 1000 Plus infrared video eye tracker (SR Research) positioned in  
218 front of the monitor. Each block began with an eye-tracking calibration and validation process. The  
219 first 9 participants underwent a 5-point calibration, while the subsequent 12 participants received a  
220 more extensive 9-point calibration. No systematic differences were observed between the two  
221 calibration groups.

222

223 Participants initiated each trial by pressing the spacebar, allowing a self-paced approach to  
224 maximize comfort and readiness. Eye gaze was continuously monitored, and trials were  
225 automatically restarted if gaze deviation exceeded 2 degrees from the fixation point for more than  
226 50 ms (3 continuous frames).

227

## 228 **Eye Movement Analysis**

229 Trials were excluded if they were shorter than 2 seconds (filling-in time [FT] < 2 seconds) to prevent  
230 accidental early responses, if median gaze displacement exceeded 1 degree from the fixation cross,  
231 or if a blink or a large saccade (velocity > 30 degrees/second velocity, detected automatically by  
232 the EyeLink control computer) occurred within 300 ms before the button press. The 300-ms cutoff  
233 was crucial to exclude ocular events potentially related to motor execution rather than visual  
234 perception. Of 7560 main trials, 6712 met these criteria and were analyzed further.

235

236 Microsaccades were detected using a refined velocity-based algorithm adapted from Engbert &  
237 Kliegl (2003). Eye gaze data from each trial were converted into visual angle velocity using a 31-  
238 ms sliding window. To minimize artifacts, data within 150 ms before and after each blink were  
239 excluded. Microsaccades were identified as sequences where, for at least eight consecutive

240 timepoints, velocity exceeded a threshold based on the standard deviation above noise (Engbert &  
241 Kliegl, 2003) in both eyes (binocular detection). Microsaccades separated by less than 12 ms were  
242 merged into a single event. Additional criteria required that eye movement direction did not vary  
243 by more than 15 degrees per millisecond and that the total amplitude fell between 3 arcmin and 2  
244 degrees. Eye movements smaller than 3 arcmin were classified as ocular drift or noise, while  
245 movements larger than 2 degrees were classified as large saccades.

246

247 To determine the optimal noise threshold for each participant, we manually reviewed detected  
248 microsaccades in every trial. The thresholds for noise multipliers were calibrated based on trial-by-  
249 trial manual review to ensure accuracy in detecting true microsaccades versus noise. Eighteen  
250 participants were assigned a noise multiplier of 5, while three required a multiplier of 6.

251

252 To qualitatively examine microsaccade dynamics in relation to perceptual filling-in, we assembled  
253 a vector of microsaccade onsets for each trial, aligning the spacebar press (indicating filling-in) to  
254 time zero. These vectors were summed across trials to calculate microsaccade frequency as a rate  
255 per second, using a causal windowing function (Engbert, 2006) with a window length of 1001 ms  
256 and an alpha value of 1/100—similar to methods used in neuronal firing rate analysis (Dayan &  
257 Abbott, 2001). Trials with blinks or large saccade within 2 seconds of the button press were  
258 excluded (543 excluded trials). For visualization, we normalized microsaccade rates so that each  
259 participant's average rate during the baseline period (-5 to -3 seconds before button press) matched  
260 the study population's average baseline rate.

261

262 Ocular drift was measured using the “retinal slip” methodology (Engbert & Mergenthaler, 2006),  
263 which calculates the distance of gaze traversal in visual angle over time. The screen was divided  
264 into a grid of 0.01 x 0.01-degree squares, approximately representing the diameter of a cone's  
265 receptive field. We tracked the number of squares traversed in each 50-ms segment of a trial,  
266 converting the count into a rate of degrees per second. Timepoints during or immediately (10 ms)  
267 before or after a microsaccade were excluded to isolate ocular drift from microsaccadic movements.

268

### 269 **Linear Mixed Modeling of Filling-in Time**

270 We used linear mixed models to predict the time taken for perceptual filling-in in each trial,  
271 considering various stimulus attributes and eye movements. The models were built using the *lme4*  
272 *v11.1.35.1* package (Bates et al., 2015) in *R Statistical Software v4.3.2* (R Core Team, 2023). Our



273 approach involved systematic model construction and parameter selection, testing specific  
274 hypotheses without overcomplicating the models.

275

276 Filling-in times (FT) were log-transformed to improve model fitting. Continuous predictor variables  
277 were standardized by zero-centering and scaling by their standard deviations. We used restricted  
278 maximum likelihood estimation (REML) with the *BOBYQA* optimization algorithm for model  
279 fitting. Parameters were considered statistically significant if their Bonferroni-corrected confidence  
280 intervals (excluding the intercept) did not include 0 (see *Statistical Analysis*). Post-hoc analyses  
281 were performed to determine if removing them improved model fit, as indicated by a lower  
282 Bayesian information criterion (BIC). Parameters whose removal did not improve model fit were  
283 retained for inclusion in future models.

284

285 Model A (Table S1) was designed to predict FT based solely on stimulus properties, without  
286 considering eye movements. Included trial-by-trial variables were stimulus contrast, eccentricity,  
287 and trial number, which helped assess any changes in FT across the block. The *lme4* syntax was  
288 defined as:

289 
$$FT \sim (\text{contrast} + \text{eccentricity} + \text{trial\_num} \mid \text{participant}) + \text{contrast} + \text{eccentricity} +$$
  
290 
$$\text{trial\_num} + \text{contrast}:\text{eccentricity} + \text{contrast}:\text{trial\_num} + \text{eccentricity}:\text{trial\_num}.$$

291

292 Model B (Table S2) incorporated the significant parameters from Model A, adding main effects of  
293 four eye movement variables: microsaccade presence (whether microsaccades occurred during a  
294 trial), number of blinks, and average ocular drift. We focused on microsaccade presence (rather  
295 than count or rate) for two reasons: 1) to determine if microsaccades prolonged FT in general, and  
296 how this effect interacted with contrast or eccentricity, and 2) to avoid potential spurious  
297 correlations between longer trial durations and increased spontaneous eye movements, which are  
298 challenging to interpret. The *lme4* syntax for Model B was:

299 
$$FT \sim (\text{contrast} + \text{eccentricity} + \text{trial\_num} + \text{ms\_presence} + \text{num\_blinks} +$$
  
300 
$$\text{ocular\_drift} \mid \text{participant}) + \text{contrast} + \text{eccentricity} + \text{trial\_num} +$$
  
301 
$$\text{contrast}:\text{trial\_num} + \text{ms\_presence} + \text{num\_blinks} + \text{ocular\_drift}$$

302

303 The primary model (Table 1) included fixed and random main effect variables identified from  
304 Model B, plus their fixed-effect interactions. The critical tests of interest were the interaction effects  
305 between microsaccade presence and stimulus contrast or eccentricity. The *lme4* syntax was:

306  $FT \sim (\text{contrast} + \text{eccentricity} + \text{trial\_num} + \text{ms\_presence} + \text{num\_blinks} /$   
307  $\text{participant}) + \text{contrast} + \text{eccentricity} + \text{trial\_num} + \text{contrast:trial\_num} +$   
308  $\text{ms\_presence} + \text{num\_blinks} + \text{ms\_presence:contrast} + \text{ms\_presence:eccentricity} +$   
309  $\text{num\_blinks:contrast} + \text{num\_blinks:eccentricity}$

310

311 Two additional models (Table 2) were used to further verify whether the effects of contrast and  
312 eccentricity on FT depended on microsaccade occurrence. We separately analyzed trials without  
313 any microsaccades or blinks and trials with at least one microsaccade but no blinks. To balance trial  
314 counts across both models for each participant, we randomly excluded trials from the model that  
315 contained more trials, resulting in 630 total trials for each model (9.4% of the total). Both models  
316 used the following *lme4* syntax:

317  $FT \sim (1 | \text{participant}) + \text{contrast} + \text{eccentricity} + \text{trial\_num} + \text{ocular\_drift}$

318 Given the reduced trial counts, random slopes were not fitted, and we used uncorrected 95%  
319 confidence intervals to minimize the risk of false negatives.

320

### 321 **Linear Mixed Modeling of Microsaccade Generation**

322 We evaluated the influence of boundary contrast, eccentricity, and trial number on microsaccade  
323 generation, measured as the trial-wise microsaccade rate. The model was formulated in *lme4* syntax  
324 as:

325  $\text{ms\_rate} \sim (\text{contrast} + \text{eccentricity} + \text{trial\_num} | \text{participant}) + \text{contrast} +$   
326  $\text{eccentricity} + \text{trial\_num}$

327

### 328 **Linear Mixed Modeling of Immobilization Time**

329 We also conducted linear mixed modeling to analyze immobilization time, defined as the duration  
330 between the last microsaccade in a trial and the button press indicating perceptual filling-in. To  
331 ensure relevance to the perceptual experience, we included only trials where the last microsaccade  
332 occurred more than 300 ms before the button press (4692 trials). This criterion was crucial to  
333 exclude eye movements that might occur after the perceptual event but before the motor response,  
334 which could potentially confound our analysis (Betta & Turatto, 2006). The model for  
335 immobilization time was structured as:

336  $\text{immobilization\_time} \sim (\text{contrast} + \text{eccentricity} + \text{ms\_amplitude} + \text{trial\_num} /$   
337  $\text{participant}) + \text{contrast} + \text{eccentricity} + \text{ms\_amplitude} + \text{trial\_num}$

338

## 339 **Statistical Analysis**

340 Average filling-in times for main trials and “sharp” catch trials were compared using a Wilcoxon  
341 signed-rank test. To determine the statistical significance of fixed effect parameters in all linear  
342 mixed models, we used case-bootstrapping with the *lmeresampler v0.2.4 R* package (Loy et al.,  
343 2023). This approach was chosen because it validates parameter estimates with minimal  
344 assumptions regarding data distribution (Leeden et al., 2008). By resampling participants’ data  
345 with replacement, we could derive more robust confidence intervals for each fixed effect  
346 parameter, thus improving the reliability of our inferences about microsaccadic effects. For each  
347 model, we performed 10,000 resampling iterations, resampling individual participants’ data with  
348 replacement, to derive percentile confidence intervals for each fixed effect parameter.

349

350

## 351 **Results**

352

### 353 **Both Eccentricity and Color Contrast Prolong Filling-in Time**

354 Twenty-one human participants completed a perceptual task to assess isoluminant color filling-in  
355 across the boundary between a central disk and its surrounding periphery (Fig. 1a). Filling-in was  
356 reported in the majority of main trials ( $95.4\% \pm 4.75$ ; mean  $\pm$  standard deviation across  
357 participants), with an average filling-in time (FT) of  $7.51 \pm 0.48$  seconds (mean  $\pm$  standard error).

358

359 The results showed a clear relationship between boundary strength and filling-in time (FT). Both  
360 higher color contrast and lower eccentricity boundaries increased FT (Fig. 1b, 1c; Table S1; linear  
361 mixed modeling,  $\alpha = 0.0083$ ). No significant interaction was found between color contrast and  
362 eccentricity in their effects on FT. A trend was also observed where FT decreased as the task block  
363 progressed, and the effect of color contrast on FT diminished over time (Table S1).

364

365

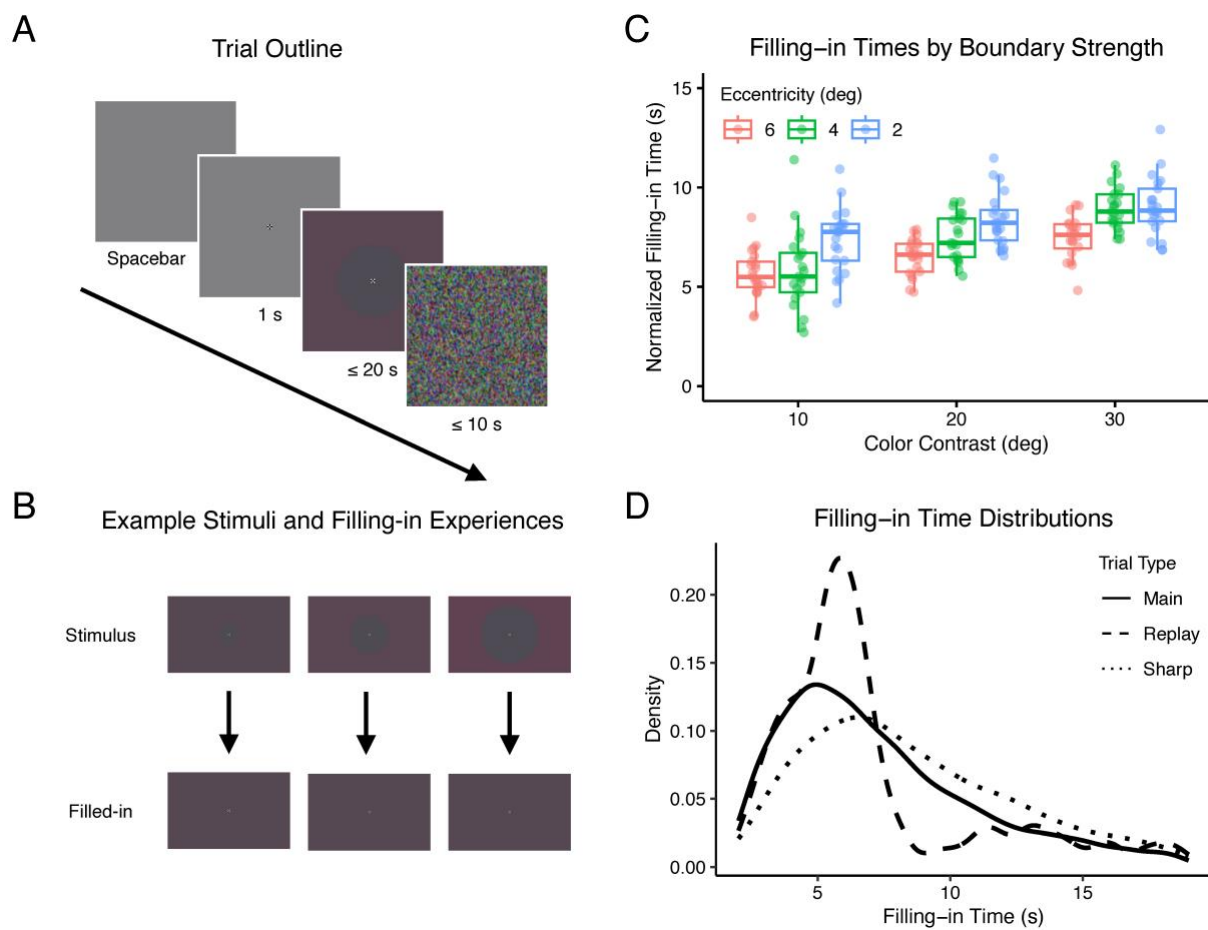


**Fig. 1. Experiment Design and Behavior**

**(A) Sequence of events in a typical trial.** Participants initiated each trial by pressing the spacebar, and the visual stimulus persisted until a second spacebar press or a maximum of 20 seconds elapsed. Dynamic noise followed each trial to mitigate retinal afterimages.

**(B) Stimulus transition and perceptual effect.** The stimulus included a central disk varying in radius and with three possible color contrasts (top row). After boundary fading, the central and peripheral regions perceptually merged, creating a uniform color field (bottom row).

**(C) Normalized filling-in time across main trials.** plotted against the boundary's color contrast and eccentricity. Each data point represents an individual participant's experience. Boxplots show median, 25<sup>th</sup> and 75<sup>th</sup> percentiles across individual subject means.

**(D) Distribution of filling-in times across different trial types.** Control trials with sharp boundaries (dotted line) typically resulted in prolonged FT compared to main trials (solid line), while replay trials (dashed line) showed clustered FT around the simulated effect (6-8 seconds).

366

367 In the 45 controlled “replay” catch trials, FT was concentrated around the time when the stimulus  
 368 became visually uniform (6-8 seconds; Fig. 1d), with reduced variability across stimulus conditions  
 369 (Fig. S1a). In the set of 45 “sharp” trials intended to extend filling-in time, FT exceeded that of  
 370 main trials for all participants ( $9.12 \pm 0.55$  seconds; Wilcoxon signed-rank test,  $W = 0$ ,  $p < 0.001$ ,  
 371 Fig. 1d), across all stimulus conditions (Fig. S1b). The consistent results across replay and sharp  
 372 trials indicate that participants' responses accurately reflected their perceptual experience of filling-  
 373 in.

374

## 375 **Eccentricity Only Predicts Filling-in time When Microsaccades Occur**

376 The primary analysis confirmed two key assumptions regarding microsaccade behavior: 1) detected  
377 microsaccades conformed to the classic “main sequence” relationship, which describes the  
378 correlation between magnitude and peak velocity (Bahill et al., 1975; Fig. 2a), and 2) microsaccade  
379 rate exhibited a notable dip approximately 600 ms before participants reported perceptual filling-in  
380 (Costela et al., 2017; Martinez-Conde et al., 2006; McCamy et al., 2012; Troncoso et al., 2008; Fig.  
381 2b). Microsaccade rate profiles remained consistent across all nine stimulus conditions (three levels  
382 of color contrast and three levels of eccentricity), with no significant deviations beyond random  
383 variation (detailed rate curves in Fig. S2).

384  
385 The comprehensive linear mixed model outcomes, with bootstrap-derived confidence intervals ( $\alpha$   
386 = 0.005), are detailed in Table 1 (see Tables S1 and S2 for precursor models used for parameter  
387 selection). Our findings demonstrate that filling-in time was significantly prolonged in trials where  
388 microsaccades occurred, as well as in trials with increased blinks. Among the interactions between  
389 stimulus properties and ocular movements, the interaction between microsaccade presence and  
390 boundary eccentricity was the only significant effect. Specifically, the impact of boundary  
391 eccentricity on FT was significantly amplified in the presence of microsaccades, while color  
392 independently influenced FT. These findings remained consistent when recalibrating eccentricity  
393 values using a logarithmic conversion based on cortical magnification. This conversion translates  
394 visual field eccentricity ( $E$ ) into cortical distance ( $d$ , in mm) from the retinotopic representation  
395 corresponding to 10 degrees of visual angle (Engel et al., 1997):  $d = \log(E) / 0.063 - 36.54$ .

396

397

398 **Table 1. Fixed effects from a linear mixed-effect model of log-transformed filling-in time.**

<b>Parameter</b>	<b>Estimate</b>	<b>99.5% Percentile CI</b>
intercept	0.310	0.129, 0.479
contrast	0.115	<b>0.0369, 0.172 *</b>
eccentricity	-0.00939	-0.0606, 0.0536
ms_presence	0.302	<b>0.173, 0.455 *</b>
num_blinks	0.265	<b>0.265, 0.203 *</b>
trial_num	-0.101	<b>-0.121, -0.0829 *</b>
contrast : trial	-0.0152	-0.0318, 0.000583
ms_presence : contrast	-0.00757	-0.0584, 0.0552

ms_presence : eccentricity	-0.0715	<b>-0.137, -0.0251 *</b>
num_blinks : contrast	-0.0160	-0.0587, 0.0320
num_blinks : eccentricity	0.0126	-0.0321, 0.0383

399 \*: the percentile bootstrap confidence interval (CI), Bonferroni-corrected across fixed effect parameters, does not  
400 contain 0 ( $\alpha = 0.005$ ). The intercept is presented for reference but not evaluated for statistical significance.

401

402 We further examined whether boundary strength, manipulated through color contrast and  
403 eccentricity, influenced perceptual filling-in time independently of microsaccades. Trials were  
404 divided based on ocular stability: those with no microsaccades or blinks, and those with at least one  
405 microsaccade but no blinks. As hypothesized, both color contrast and eccentricity significantly  
406 predicted FT in trials where microsaccades occurred (Table 2, left column; Fig. 2c-d;  $\alpha = 0.05$ ).  
407 Interestingly, in trials without microsaccades—indicating stable fixation—eccentricity had no  
408 effect on FT (Table 2, right column; Fig. 2d). However, color contrast continued to predict FT even  
409 under stable fixation (Fig. 2c).

410

411 To test an alternative hypothesis—that stronger visual boundaries prolong FT by increasing the rate  
412 of microsaccade generation rather than their efficacy—we analyzed the relationship between  
413 microsaccade rate and boundary properties. Contrary to this hypothesis, we found no significant  
414 association between microsaccades rate and either color contrast or eccentricity (Table 3; Fig. 3a;  
415  $\alpha = 0.0167$ ).

416

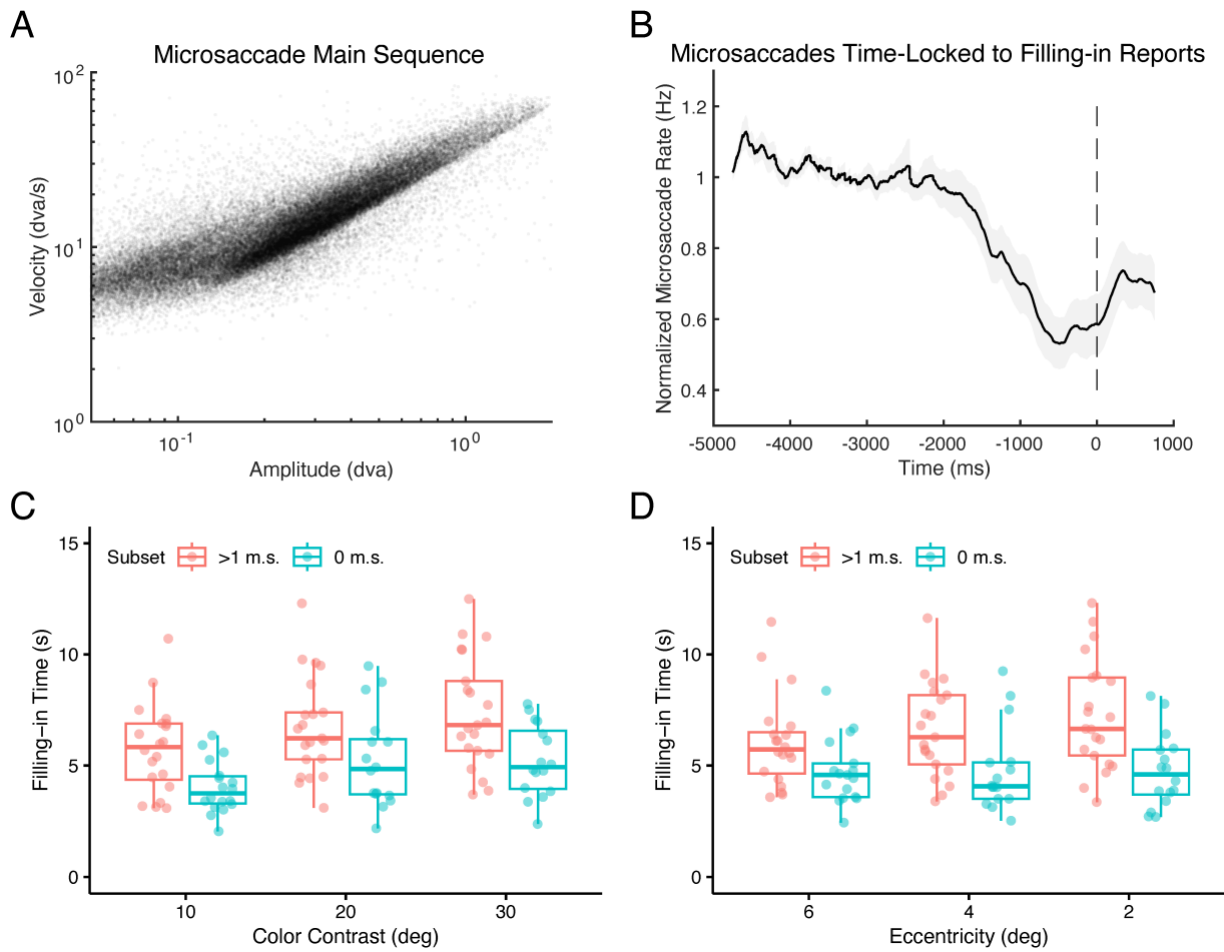


**Fig. 2. Microsaccade Dynamics and Their Influence on Filling-in Time**

(A) Relationship between amplitude and peak velocity of individual microsaccades during main trials, demonstrating adherence to the classic main sequence relationship.

(B) Average normalized microsaccade rate in the period leading up to participants' report of perceptual filling-in.

(C) Filling-in time as a function of color contrast, comparing trials with at least one microsaccade (red) to trials without microsaccades (blue).

(D) Filling-in time as a function of boundary eccentricity, comparing trials with at least one microsaccade (red) to trials without microsaccades (blue). Each data point represents an individual participant. Boxplots show the median, 25<sup>th</sup>, and 75<sup>th</sup> percentiles of participants' means.

417

418

419

420

421

422

423

424

425

426

427

428 **Table 2. Fixed effects from a comparative linear mixed-effect model analysis of**  
 429 **microsaccade-dependent filling-in time.**

Parameter	microsaccade trials		no-microsaccade trials	
	Estimate	95% Percentile CI	Estimate	95% Percentile CI
intercept	0.498	0.363, 0.620	0.176	0.0636, 0.279
contrast	0.156	<b>0.0941, 0.202 *</b>	0.166	<b>0.0851, 0.225 *</b>
eccentricity	-0.0876	<b>-0.131, -0.0350 *</b>	-0.00389	-0.0305, 0.0310
trial_num	-0.101	<b>-0.130, -0.0722 *</b>	-0.0762	<b>-0.100, -0.0552 *</b>
ocular_drift	0.104	<b>0.000418, 0.170 *</b>	0.0453	<b>0.0183, 0.129 *</b>

430 Linear mixed models evaluated filling-in time (FT) in two distinct subsets of trials: those with at least one  
 431 microsaccade occurring (630 trials, left columns) and those devoid of microsaccades (630 trials, right columns).

432 \*: the percentile bootstrap confidence interval (CI) does not contain 0 ( $\alpha = 0.05$ ). The intercept is presented for  
 433 reference but not evaluated for statistical significance.

434

### 435 **Eccentricity, but Not Color Contrast, Influences Microsaccadic Efficacy**

436 Another way to evaluate microsaccade efficacy is to quantify the additional fixation time required  
 437 for perceptual filling-in following each microsaccade. According to slow adaptation hypotheses of  
 438 boundary fading, neural signals gradually diminish until the visual boundary fades from perception.  
 439 Microsaccades counteract this adaptation by restoring part of the diminished signal, delaying fading  
 440 and subsequent filling-in. The amount of signal restoration—and hence the delay—would be  
 441 expected to increase with more effective microsaccades, such as those occurring at smaller  
 442 boundary eccentricities. Although we cannot determine the exact microsaccade-induced delay or  
 443 signal increment, we can infer how reduced eccentricity extends this delay by analyzing  
 444 “immobilization time”—the duration from the last microsaccade to the report of filling-in, reflecting  
 445 the time the eyes must remain stationary for filling-in to occur.

446

447 As hypothesized, immobilization time was significantly associated with eccentricity but not with  
 448 color contrast, as revealed by a linear mixed model (Table 4; Fig. 3b;  $\alpha = 0.0167$ ). Average  
 449 immobilization times were  $2220 \pm 242$  ms for the 2-degree eccentricity condition,  $2057 \pm 229$  ms  
 450 for 4 degrees, and  $1903 \pm 184$  ms for 6 degrees. Interestingly, the amplitude of the last microsaccade  
 451 did not predict immobilization time, suggesting that the extent of retinal image displacement does  
 452 not directly affect microsaccade efficacy in delaying filling-in. Immobilization times also tended to  
 453 decrease as trials progressed within a block. It is important to note that the reported immobilization



454 times include not only the delay induced by microsaccades but also any residual adaptation period  
 455 and motor response time.

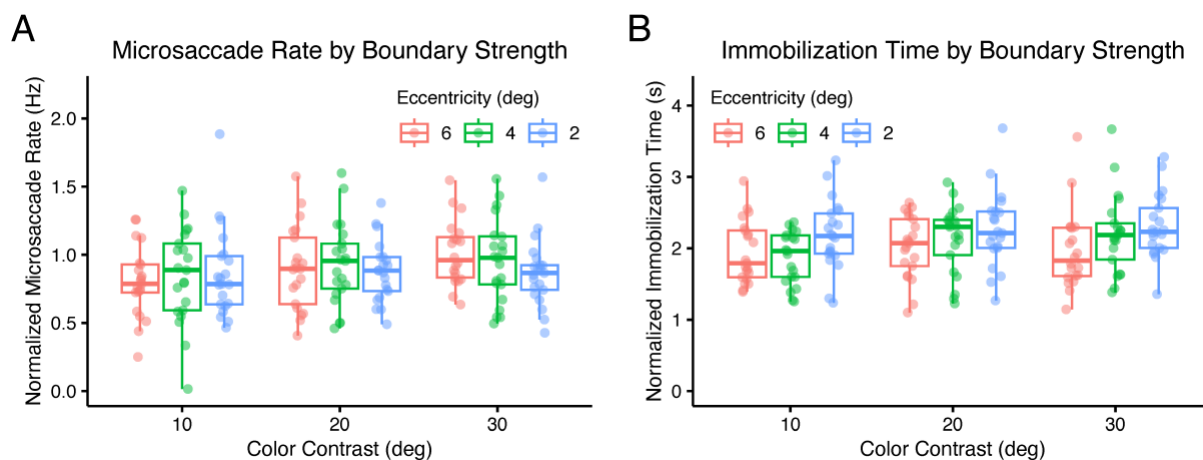


**Fig. 3. Microsaccade Rates and Immobilization Times in Relation to Visual Stimulus Parameters**

(A) Normalized microsaccade rate throughout trials as a function of color contrast and boundary eccentricity.  
 (B) Normalized immobilization time as a function of color contrast and boundary eccentricity. Immobilization time represents the duration of stable fixation after the last microsaccade until the report of perceptual filling-in. Each data point represents an individual participant. Boxplots show the median, 25<sup>th</sup>, and 75<sup>th</sup> percentiles across participants' means.

456  
 457  
 458  
 459  
 460

**Table 3. Fixed effects from a linear mixed-effect model of log-transformed microsaccade rate.**

Parameter	Estimate	98.33% Percentile CI
intercept	-0.0845	-0.307, 0.128
contrast	-0.000870	-0.0449, 0.0426
eccentricity	0.0350	-0.00397, 0.0723
trial_num	0.134	<b>0.0893, 0.175 *</b>

461 \*: the percentile bootstrap confidence interval (CI), Bonferroni-corrected across fixed effect parameters, does not  
 462 contain 0 ( $\alpha = 0.0167$ ). The intercept is presented for reference but not evaluated for statistical significance.

463  
 464  
 465

466  
467  
468  
469  
470

**Table 4. Fixed effects from a linear mixed-effect model of log-transformed immobilization time.**

<b>Parameter</b>	<b>Estimate</b>	<b>98.33% Percentile CI</b>
intercept	-0.165	-0.379, 0.0410
contrast	0.0283	-0.00232, 0.0599
eccentricity	-0.0587	<b>-0.0937, -0.0242 *</b>
trial_num	-0.105	<b>-0.134, -0.0739 *</b>
ms_amplitude	0.0110	-0.0272, 0.0406

471 \*: the percentile bootstrap confidence interval (CI), Bonferroni-corrected across fixed effect parameters, does not  
472 contain 0 ( $\alpha = 0.0167$ ). The intercept is presented for reference but not evaluated for statistical significance.

473  
474

## 475 Discussion

476 During voluntary gaze fixation, microsaccades play a crucial role in maintaining visual perception  
477 by preventing the fading of visual boundaries that would otherwise lead to perceptual filling-in.  
478 Despite their significance, the mechanisms underlying how microsaccades modulate this process  
479 remain poorly understood. This study demonstrates that the efficacy of microsaccades in delaying  
480 perceptual filling-in is influenced by retinal eccentricity but is independent of color contrast,  
481 offering new insights into the mechanisms of perceptual stability. Specifically, we found that higher  
482 color contrast independently increased the time required for perceptual filling-in (filling-in time,  
483 FT), while microsaccades mitigated boundary fading equally across varying contrast levels.  
484 Conversely, lower boundary eccentricity increased the efficacy of microsaccades, whereas FT  
485 remained consistent across different eccentricities when no microsaccades were present. These  
486 conclusions were supported by a series of linear mixed model analyses that revealed: 1) a significant  
487 interaction between microsaccade occurrence and boundary eccentricity, but not color contrast, in  
488 predicting FT; 2) a significant effect of eccentricity on FT when microsaccades were present, but  
489 not in trials without microsaccades; and 3) a significant impact of eccentricity, but not color  
490 contrast, on immobilization time—the stable fixation period between the last microsaccade and the  
491 report of filling-in.

492

493 The lack of sensitivity of FT to eccentricity in the absence of microsaccades, despite the established  
494 relationships between eccentricity, visual acuity, and cortical magnification (Duncan & Boynton,  
495 2003), suggests that visual adaptation of boundaries may occur uniformly across the visual field.

496 This finding aligns with previous studies (Bachy & Zaidi, 2014a; Greenlee et al., 1991) but  
497 highlights an indirect role of eccentricity in modulating the impact of microsaccades on adaptation.

498  
499 Two secondary findings emerged regarding the progression of trials within each block. First, we  
500 observed a decrease in both filling-in time and immobilization time as trials progressed, which we  
501 attribute to practice effects resulting in faster motor responses. Second, we found that the effect of  
502 trial number on FT exhibited a negative interaction with color contrast, suggesting that the influence  
503 of contrast on FT diminished over time. Although this interaction did not meet the strict statistical  
504 threshold, excluding it from the model led to poorer performance, suggesting its potential relevance.  
505 One plausible explanation is that visual neurons gradually adapt to the higher-level, sustained visual  
506 context of a trial block, normalizing their responses over time (Webster, 2011).

507  
508 Our study provides significant new insight into the mechanisms underlying microsaccades' role in  
509 perceptual filling-in. We demonstrated that microsaccades do not simply resample the initial visual  
510 stimulus, as their efficacy in preventing filling-in varies with boundary eccentricity but is unaffected  
511 by color contrast. This finding suggests that microsaccades serve a more complex role than merely  
512 refreshing the visual input. The relationship between microsaccade efficacy and eccentricity can  
513 likely be attributed to cortical magnification and receptive field size—stimuli at higher  
514 eccentricities are processed by fewer cortical neurons with larger receptive field sizes (Daniel &  
515 Whitteridge, 1961). Consequently, at higher eccentricities fewer neurons are activated by the subtle  
516 retinal shifts induced by microsaccades (Donner & Hemilä, 2007). This hypothesis has been  
517 proposed previously (Clarke & Belcher, 1962) and could also be related to variations in retinal  
518 ganglion cell responses across eccentricities (Bachy & Zaidi, 2014b). These findings imply that  
519 certain visual field asymmetries in behavior may be entirely due to fixational eye movement  
520 dynamics. This could be of clinical relevance for optimizing visual rehabilitation strategies for  
521 individuals with central vision loss or age-related macular degeneration, where enhancing the  
522 stability of central visual representations is critical.

523  
524 Interestingly, we found no correlation between microsaccade amplitude and efficacy. While larger  
525 amplitude microsaccades would theoretically stimulate more neurons, we found that this broader  
526 stimulation does not necessarily enhance filling-in prevention, consistent with prior findings  
527 (McCamy et al., 2014). It is possible that the critical neural population consists of cells with  
528 receptive fields at the boundary before or after a microsaccade, rather than all cells activated during  
529 the eye movement. Alternatively, the concept of corollary discharge, in which microsaccade

530 generation modulates gain in visual cortex before the movement occurs (Chen et al., 2015), could  
531 offer a mechanism for the refreshing effect of microsaccades. This boost may be more pronounced  
532 at smaller eccentricities due to cortical magnification and may not vary with contrast. If this is the  
533 case, the actual retinal image shift may be irrelevant to boundary fading—an intriguing hypothesis  
534 that warrants further investigation.

535

536 We also found that microsaccade efficacy was insensitive to isoluminant color contrast, reinforcing  
537 the idea that microsaccades do not simply replicate the initial visual stimulus. This suggests that  
538 the feature defining the visual boundary and its adaptation dynamics does not modulate how  
539 microsaccades prevent such adaptation. Future research should investigate whether this invariance  
540 to color contrast extends to other visual properties, such as luminance. Such work would be essential  
541 for delineating the neural processes and brain regions involved in adaptation and microsaccadic  
542 counteraction. Given that neurons in the primary visual cortex (V1) process contours formed from  
543 both luminance and isoluminant color edges similarly (De & Horwitz, 2022; Hamburger et al.,  
544 2007), it seems unlikely that microsaccadic efficacy would vary based on these properties. Instead,  
545 the mechanism may originate in motion-processing pathways, which are known to be invariant to  
546 luminance and color contrast for rapid retinal motion (Hawken et al., 1994), or through corollary  
547 discharge as discussed.

548

549 Our experimental design has certain limitations. Trials within each block were not randomized by  
550 contrast and eccentricity, potentially introducing non-stimulus-related effects, such as arousal  
551 fluctuations. However, the consistent relationship between FT and both contrast and eccentricity  
552 across participants makes this unlikely. Additionally, although replay control trials verified task  
553 accuracy, they did not fully mimic the gradual perceptual filling-in experience. Sudden changes in  
554 physical contrast can abruptly remove stimuli from conscious perception (May et al., 2003) due to  
555 normalization of neuronal firing rates to the current visual input. A reduction of neural firing below  
556 baseline can even produce opposite afterimages (Bachy & Zaidi, 2014a, 2014b), which would  
557 further differentiate the replay and filling-in experiences. Indeed, participants often reported the  
558 replay stimulus as inverting—first appearing uniform and then revealing the center disk in the  
559 opposite color. Nevertheless, our intention for including a replay condition was only to verify task  
560 engagement.

561

562 Lastly, the narrow range of color contrasts sampled may have limited our ability to detect subtle  
563 relationships between contrast and microsaccades. Although our findings suggest that any potential

564 contrast effect on microsaccadic adaptation prevention is minimal compared to the effect on  
565 adaptation itself, further research using a broader contrast range is needed. Moreover, the industry-  
566 standard eye tracker used may not detect the smallest microsaccades (<15 arcmin; Collewijn &  
567 Kowler, 2008). Although trials without detected microsaccades were labeled accordingly, it is  
568 possible that undetected eye movements were present. Even so, our robust findings suggest that  
569 such small movements would be ineffective at preventing filling-in, raising the question of whether  
570 a minimum microsaccade magnitude is required to influence boundary fading.

## 573 **Conclusions**

574 The present findings shed light on how fixational eye movements modulate the initial stage of  
575 perceptual filling-in—boundary fading. While higher color contrast inherently increases filling-in  
576 time, microsaccades specifically mediate the similar influence of boundary eccentricity. This  
577 suggests that microsaccades prevent boundary fading via transient boundary stimulation that scales  
578 with cortical magnification but is invariant to boundary contrast. Together, these findings offer a  
579 foundation for future research aimed at identifying the precise neurophysiological mechanisms  
580 underlying the interaction between eye movements and visual perception, with potential  
581 applications in both clinical and technological domains.

584 **References**

- 585 Bachy, R., & Zaidi, Q. (2014a). Factors governing the speed of color adaptation in foveal versus  
586 peripheral vision. *Journal of the Optical Society of America A*, *31*(4), A220–A225.  
587 <https://doi.org/10.1364/JOSAA.31.00A220>
- 588 Bachy, R., & Zaidi, Q. (2014b). Troxler Fading, Eye Movements, and Retinal Ganglion Cell  
589 Properties. *I-Perception*, *5*(7), 611–612. <https://doi.org/10.1068/i0679sas>
- 590 Bahill, A. T., Clark, M. R., & Stark, L. (1975). The main sequence, a tool for studying human eye  
591 movements. *Mathematical Biosciences*, *24*(3), 191–204. [https://doi.org/10.1016/0025-  
592 5564\(75\)90075-9](https://doi.org/10.1016/0025-5564(75)90075-9)
- 593 Bates, D., Mächler, M., Bolker, B., & Walker, S. (2015). Fitting Linear Mixed-Effects Models  
594 Using lme4. *Journal of Statistical Software*, *67*(1), 1–48.  
595 <https://doi.org/10.18637/jss.v067.i01>
- 596 Betta, E., & Turatto, M. (2006). Are you ready? I can tell by looking at your microsaccades.  
597 *Neuroreport*, *17*, 1001–1004. <https://doi.org/10.1097/01.wnr.0000223392.82198.6d>
- 598 Brainard, D. H. (1997). The Psychophysics Toolbox. *Spatial Vision*, *10*(4), 433–436.  
599 <https://doi.org/10.1163/156856897X00357>
- 600 Chen, C.-Y., Ignashchenkova, A., Thier, P., & Hafed, Z. M. (2015). Neuronal Response Gain  
601 Enhancement prior to Microsaccades. *Current Biology*, *25*(16), 2065–2074.  
602 <https://doi.org/10.1016/j.cub.2015.06.022>
- 603 Clarke, F. J. J., & Belcher, S. J. (1962). On the localization of troxler’s effect in the visual  
604 pathway. *Vision Research*, *2*(1), 53–68. [https://doi.org/10.1016/0042-6989\(62\)90063-9](https://doi.org/10.1016/0042-6989(62)90063-9)
- 605 Collewijn, H., & Kowler, E. (2008). The significance of microsaccades for vision and oculomotor  
606 control. *Journal of Vision*, *8*(14), 20.1-21. <https://doi.org/10.1167/8.14.20>
- 607 Costela, F. M., McCamy, M. B., Coffelt, M., Otero-Millan, J., Macknik, S. L., & Martinez-  
608 Conde, S. (2017). Changes in visibility as a function of spatial frequency and

- 609            microsaccade occurrence. *European Journal of Neuroscience*, 45(3), 433–439.
- 610            <https://doi.org/10.1111/ejn.13487>
- 611 Daniel, P. M., & Whitteridge, D. (1961). The representation of the visual field on the cerebral  
612            cortex in monkeys. *The Journal of Physiology*, 159(2), 203–221.
- 613 Dayan, P., & Abbott, L. F. (2001). *Theoretical Neuroscience: Computational and Mathematical*  
614            *Modeling of Neural Systems*. MIT Press.
- 615 De, A., & Horwitz, G. D. (2022). Coding of chromatic spatial contrast by macaque V1 neurons.  
616            *eLife*, 11, e68133. <https://doi.org/10.7554/eLife.68133>
- 617 De Weerd, P., Desimone, R., & Ungerleider, L. G. (1998). Perceptual filling-in: A parametric  
618            study. *Vision Research*, 38(18), 2721–2734. [https://doi.org/10.1016/S0042-](https://doi.org/10.1016/S0042-6989(97)00432-X)  
619            [6989\(97\)00432-X](https://doi.org/10.1016/S0042-6989(97)00432-X)
- 620 Derrington, A. M., Krauskopf, J., & Lennie, P. (1984). Chromatic mechanisms in lateral  
621            geniculate nucleus of macaque. *The Journal of Physiology*, 357, 241–265.  
622            <https://doi.org/10.1113/jphysiol.1984.sp015499>
- 623 Donner, K., & Hemilä, S. (2007). Modelling the effect of microsaccades on retinal responses to  
624            stationary contrast patterns. *Vision Research*, 47(9), 1166–1177.  
625            <https://doi.org/10.1016/j.visres.2006.11.024>
- 626 Duncan, R. O., & Boynton, G. M. (2003). Cortical Magnification within Human Primary Visual  
627            Cortex Correlates with Acuity Thresholds. *Neuron*, 38(4), 659–671.  
628            [https://doi.org/10.1016/S0896-6273\(03\)00265-4](https://doi.org/10.1016/S0896-6273(03)00265-4)
- 629 Engbert, R. (2006). Microsaccades: A microcosm for research on oculomotor control, attention,  
630            and visual perception. In S. Martinez-Conde, S. L. Macknik, L. M. Martinez, J.-M.  
631            Alonso, & P. U. Tse (Eds.), *Progress in Brain Research* (Vol. 154, pp. 177–192).  
632            Elsevier. [https://doi.org/10.1016/S0079-6123\(06\)54009-9](https://doi.org/10.1016/S0079-6123(06)54009-9)

- 633 Engbert, R., & Kliegl, R. (2003). Microsaccades uncover the orientation of covert attention.  
634 *Vision Research*, 43(9), 1035–1045. [https://doi.org/10.1016/S0042-6989\(03\)00084-1](https://doi.org/10.1016/S0042-6989(03)00084-1)
- 635 Engbert, R., & Mergenthaler, K. (2006). Microsaccades are triggered by low retinal image slip.  
636 *Proceedings of the National Academy of Sciences*, 103(18), 7192–7197.  
637 <https://doi.org/10.1073/pnas.0509557103>
- 638 Engel, S. A., Glover, G. H., & Wandell, B. A. (1997). Retinotopic organization in human visual  
639 cortex and the spatial precision of functional MRI. *Cerebral Cortex*, 7(2), 181–192.  
640 <https://doi.org/10.1093/cercor/7.2.181>
- 641 Greenlee, M. W., Georgeson, M. A., Magnussen, S., & Harris, J. P. (1991). The time course of  
642 adaptation to spatial contrast. *Vision Research*, 31(2), 223–236.  
643 [https://doi.org/10.1016/0042-6989\(91\)90113-j](https://doi.org/10.1016/0042-6989(91)90113-j)
- 644 Hamburger, K., Hansen, T., & Gegenfurtner, K. R. (2007). Geometric-optical illusions at  
645 isoluminance. *Vision Research*, 47(26), 3276–3285.  
646 <https://doi.org/10.1016/j.visres.2007.09.004>
- 647 Hawken, M. J., Gegenfurtner, K. R., & Tang, C. (1994). Contrast dependence of colour and  
648 luminance motion mechanisms in human vision. *Nature*, 367(6460), 268–270.  
649 <https://doi.org/10.1038/367268a0>
- 650 Kohn, A. (2007). Visual adaptation: Physiology, mechanisms, and functional benefits. *Journal of*  
651 *Neurophysiology*, 97(5), 3155–3164. <https://doi.org/10.1152/jn.00086.2007>
- 652 Kowler, E., & Steinman, R. M. (1980). Small saccades serve no useful purpose: Reply to a letter  
653 by R. W. Ditchburn. *Vision Research*, 20(3), 273–276. [https://doi.org/10.1016/0042-](https://doi.org/10.1016/0042-6989(80)90113-3)  
654 [6989\(80\)90113-3](https://doi.org/10.1016/0042-6989(80)90113-3)
- 655 Leeden, R. van der, Meijer, E., & Busing, F. M. T. A. (2008). Resampling Multilevel Models. In  
656 J. de Leeuw & E. Meijer (Eds.), *Handbook of Multilevel Analysis* (pp. 401–433). Springer.  
657 [https://doi.org/10.1007/978-0-387-73186-5\\_11](https://doi.org/10.1007/978-0-387-73186-5_11)



- 658 Levinson, M., & Baillet, S. (2022). Perceptual filling-in dispels the veridicality problem of  
659 conscious perception research. *Consciousness and Cognition*, *100*, 103316.  
660 <https://doi.org/10.1016/j.concog.2022.103316>
- 661 Loy, A., Steele, S., & Korobova, J. (2023). *lmeresampler: Bootstrap Methods for Nested Linear*  
662 *Mixed-Effects Models* [Computer software]. [https://CRAN.R-](https://CRAN.R-project.org/package=lmeresampler)  
663 [project.org/package=lmeresampler](https://CRAN.R-project.org/package=lmeresampler)
- 664 Martinez-Conde, S., & Macknik, S. L. (2017). Unchanging visions: The effects and limitations of  
665 ocular stillness. *Philosophical Transactions of the Royal Society B: Biological Sciences*,  
666 *372*(1718), 20160204. <https://doi.org/10.1098/rstb.2016.0204>
- 667 Martinez-Conde, S., Macknik, S. L., Troncoso, X. G., & Dyar, T. A. (2006). Microsaccades  
668 Counteract Visual Fading during Fixation. *Neuron*, *49*(2), 297–305.  
669 <https://doi.org/10.1016/j.neuron.2005.11.033>
- 670 May, J. G., Tsiappoutas, K. M., & Flanagan, M. B. (2003). Disappearance elicited by contrast  
671 decrements. *Perception & Psychophysics*, *65*(5), 763–769.  
672 <https://doi.org/10.3758/bf03194812>
- 673 McCamy, M. B., Macknik, S. L., & Martinez-Conde, S. (2014). Different fixational eye  
674 movements mediate the prevention and the reversal of visual fading. *The Journal of*  
675 *Physiology*, *592*(19), 4381–4394. <https://doi.org/10.1113/jphysiol.2014.279059>
- 676 McCamy, M. B., Otero-Millan, J., Macknik, S. L., Yang, Y., Troncoso, X. G., Baer, S. M., Crook,  
677 S. M., & Martinez-Conde, S. (2012). Microsaccadic efficacy and contribution to foveal  
678 and peripheral vision. *Journal of Neuroscience*, *32*(27), 9194–9204.  
679 <https://doi.org/10.1523/JNEUROSCI.0515-12.2012>
- 680 Otten, M., Pinto, Y., Paffen, C. L. E., Seth, A. K., & Kanai, R. (2017). The Uniformity Illusion:  
681 Central Stimuli Can Determine Peripheral Perception. *Psychological Science*, *28*(1), 56–  
682 68. <https://doi.org/10.1177/0956797616672270>

- 683 Poletti, M., & Rucci, M. (2010). Eye movements under various conditions of image fading.  
684 *Journal of Vision*, 10(3), 6. <https://doi.org/10.1167/10.3.6>
- 685 R Core Team. (2023). *R: A Language and Environment for Statistical Computing* (Version 4.3.2)  
686 [Computer software]. R Foundation for Statistical Computing. <https://www.R-project.org/>
- 687 Rucci, M., & Poletti, M. (2015). Control and Functions of Fixational Eye Movements. *Annual*  
688 *Review of Vision Science*, 1(1), 499–518. [https://doi.org/10.1146/annurev-vision-082114-](https://doi.org/10.1146/annurev-vision-082114-035742)  
689 [035742](https://doi.org/10.1146/annurev-vision-082114-035742)
- 690 Rucci, M., & Victor, J. D. (2015). The unsteady eye: An information-processing stage, not a bug.  
691 *Trends in Neurosciences*, 38(4), 195–206. <https://doi.org/10.1016/j.tins.2015.01.005>
- 692 Thaler, L., Schütz, A. C., Goodale, M. A., & Gegenfurtner, K. R. (2013). What is the best fixation  
693 target? The effect of target shape on stability of fixational eye movements. *Vision*  
694 *Research*, 76, 31–42. <https://doi.org/10.1016/j.visres.2012.10.012>
- 695 The MathWorks Inc. (2020). *MATLAB version: 9.9.0 (R2020b)* [Computer software]. The  
696 MathWorks Inc. <https://www.mathworks.com>
- 697 Troncoso, X. G., Macknik, S. L., & Martinez-Conde, S. (2008). Microsaccades counteract  
698 perceptual filling-in. *Journal of Vision*, 8(14), 15. <https://doi.org/10.1167/8.14.15>
- 699 Webster, M. A. (2011). Adaptation and visual coding. *Journal of Vision*, 11(5), 3.  
700 <https://doi.org/10.1167/11.5.3>
- 701 Weil, R. S., & Rees, G. (2011). A new taxonomy for perceptual filling-in. *Brain Research*  
702 *Reviews*, 67(1–2), 40–55. <https://doi.org/10.1016/j.brainresrev.2010.10.004>
- 703 Westland, S. (2021). *Computational Colour Science using MATLAB 2e* [Computer software].  
704 [https://www.mathworks.com/matlabcentral/fileexchange/40640-computational-colour-](https://www.mathworks.com/matlabcentral/fileexchange/40640-computational-colour-science-using-matlab-2e)  
705 [science-using-matlab-2e](https://www.mathworks.com/matlabcentral/fileexchange/40640-computational-colour-science-using-matlab-2e)

706

707

708 **Author contributions:**

709 Conceptualization: ML, CCP, SB

710 Methodology: ML, CCP, SB

711 Software: ML

712 Resources: CCP

713 Investigation: ML

714 Formal analysis: ML

715 Data curation: ML

716 Visualization: ML

717 Project administration: ML

718 Supervision: SB

719 Writing—original draft: ML

720 Writing—review & editing: ML, CCP, SB

721 Funding acquisition: ML, SB

722

723 **Data and materials availability:** All data needed to evaluate the conclusions in the paper are  
724 available in the main text or the supplementary materials. All experimental and analysis code, raw  
725 behavioral and eyetracking data, and processed data files are available in a public repository:  
726 <https://doi.org/10.17605/OSF.IO/KVT5A>.

727

728

729

730 **List of Supplementary Materials:**

731 Figs. S1 to S2

732 Tables S1 to S2